ELSEVIER

Journal of Alloys and Compounds 303–304 (2000) 270–275

Journal of ALLOYS AND COMPOUNDS

www.elsevier.com/locate/jallcom

$ThMn_{12}$-type magnetic $ErFe_7Al_5$ and non-magnetic YFe_7Al_5 studied by X-ray and neutron diffraction

W. Schäfer[a,]*, B. Barbier[a], I. Halevy[b]

[a]*Mineralogisch-Petrologisches Institut, Bonn University, 53115 Bonn, Germany*
[b]*Physics Department, Nuclear Research Center, Negev, 84190 Beer-Sheva, Israel*

Abstract

Structure parameters and magnetic properties of ternary $ErFe_7Al_5$ and YFe_7Al_5 intermetallics have been determined by X-ray and neutron diffraction. The compounds crystallize in the $ThMn_{12}$-type structure of space group I4/mmm with 2a, 8f and 8i sites occupied by the rare earths (R), iron and aluminium, respectively, and remaining Fe and Al on 8j. Lattice constants and interatomic distances are discussed in the context with results of previously investigated $R(Fe_xAl_{1-x})_{12}$ compounds of lower iron concentrations. Around 320 K, $ErFe_7Al_5$ undergoes a magnetic phase transition into a ferrimagnetically ordered state with antiparallel orientations of Er and Fe(8f) spins within the tetragonal basis plane. The moment values are 8.4(2) μ_B and 2.9(3) μ_B at 4.2 K per Er- and Fe-ion, respectively. In YFe_7Al_5, however, no long range magnetic order is observed. © 2000 Elsevier Science S.A. All rights reserved.

Keywords: $ErFe_7Al_5$; YFe_7Al_5; Intermetallics; Magnetic structure; Magnetic moments; Neutron diffraction

---

1. Introduction

The stability regime of $ThMn_{12}$-type ternary rare earth (R) – iron – aluminium intermetallics $R(Fe_xAl_{1-x})_{12}$ extends from $x=1/3$ (RFe_4Al_8) to about $x=2/3$ (RFe_8Al_4). Fe-concentration dependent structural and magnetic characteristics have been summarized recently, based on neutron diffraction results existing so far on compounds (R=Tb, Dy, Ho, Er) with lower iron concentrations $x\leq 1/2$ [1,2]. Common findings are: Fe and Al are distributed on preferential sites with largest and smallest distances to the rare earths, respectively; structural flexibility is lost with increasing Fe concentrations; the type of magnetic order changes from weak to very strong couplings of iron and rare earth sublattices; the magnetic ordering temperatures increase from about 30 K or 120 K (RFe_4Al_8) via 60 K or 230 K (RFe_5Al_7) to uniformly 340 K (RFe_6Al_6). RFe_6Al_6 (R=Tb, Ho, Er) exhibit identical ferrimagnetic structures [3].

Now we are extending the neutron diffraction investigations of the structural and magnetic properties of $R(Fe_xAl_{1-x})_{12}$ compounds to the regime of even higher Fe-concentrations, i.e. $x>6$. Neutron diffraction is specially suited to simultaneously study atomic and magnetic long range order and relations between them. The comparison of isostructural $ErFe_7Al_5$ and YFe_7Al_5 is of special interest with respect to different magnetic interactions due to combinations of magnetically relevant transition metal sublattices (Fe) with rare earth metal sublattices of either magnetic (Er) or non-magnetic (Y) atoms. Earlier investigations on $R(Fe_xAl_{1-x})_{12}$ compounds of lower iron content revealed long range ferrimagnetic order in $ErFe_5Al_7$ [4] and short range ordered Fe clusters in YFe_5Al_7 [5].

2. Samples and experimental

The polycrystalline material was synthezised by arc melting of the constituent metallic elements under argon-atmosphere. To ensure homogeneity, the samples were turned over and remelted several times. The resultant products were wrapped in tantalum foil and annealed in evacuated quartz tubes. Evaporation control didn't identify weight losses during the preparation process. Three batches of the material were treated at a temperature of 850°C for 10, 20 and finally 30 days, respectively. Quantitative energy dispersive system analysis was used to determine the chemical composition of different phases within the

---

*Corresponding author. Forschungszentrum Jülich, MIN/ZFR, D-52425 Jülich, Germany. Tel.: +49-2461-616-024; fax: +49-2461-613-012.

E-mail address: w.schaefer@fz-juelich.de (W. Schäfer)

PII: S0925-8388(00)00672-1

different batches. As experience shows the preparation of single phase material is known to be more and more difficult with higher iron concentrations (compare [6]). The long-time annealed material was considered to be the best for the diffraction experiments. According to X-ray and neutron diffraction, $ErFe_7Al_5$ was nearly single phase contaminated only by a small amount of cubic FeAl (Fig. 1), whereas YFe_7Al_5 contained several additional contaminations not yet identified as well as an amorphous component.

Room temperature X-ray measurements on a Siemens powder diffractometer D-5000 using graphite-monochromized Cu-radiation were performed by stepscanning with $\Delta 2\Theta = 0.02°$ and measuring times of 4s per step (compare Fig. 1). Neutron diffraction patterns were collected for about 12 h at 4.2 K, 293 K and 400 K using a wavelength of 1.0926 Å. Data collection on the University of Bonn powder diffractometer SV7 installed at the FRJ-2 reactor (DIDO) in the Forschungszentrum Jülich was done with two units of the linear position-sensitive scintillation detector JULIOS [7]. Additional short-time temperature dependent measurements were performed in steps of about 25 K between 4.2 K and 400 K. The sample material was contained in cylindrical vanadium cans of about 8 mm diameter and 30 mm height. The cans were mounted alternatively in a He-refrigerator cryostat (4.2 K to 293 K) and a heater device (293 K to 400 K).

2.1. Structure results

The $ThMn_{12}$-type structure of $ErFe_7Al_5$ and YFe_7Al_5 was confirmed by Rietveld refinements of the X-ray and neutron diffraction patterns. The structure is described by the tetragonal space group I4/mmm and a unit cell containing four partial structures according to site occupations 2a (0,0,0) by Er (Y), 8f (1/4,1/4,1/4) by Fe, 8i (x,0,0) by Al, and 8j (x,1/2,0) by the remaining Fe and Al atoms (Fig. 2). Due to deviations from stoichiometry the 8j sites accommodate 60% Fe and 40% Al. In YFe_7Al_5, additionally, an occupation deficiency of about 10% Fe is observed on the 8f sites. The resultant structural parameters obtained from the refinement calculations of the 4.2 K, 293 K and 400 K patterns are compiled in Table 1. The precision of the neutron diffraction lattice constants seems fair in view of the reasonably observed thermal expansions of the unit cells by about 4 $Å^3$ from 4.2 K to 400 K. The accuracy, however, is limited by about $\Delta a \approx 0.01$ Å and $\Delta c \approx 0.02$ Å considering the observed differences of the room temperature values deduced from X-ray and neutron diffraction. Inter- and intrasublattice atomic distances of the Er-compound are summarized in Table 2 on basis of the 293 K neutron data and in comparison to corresponding values of less Fe containing Er-compounds, which had been measured earlier under similar experimental conditions on the same neutron diffractometer (compare [2]).

2.2. Magnetic results

The 4.2 K pattern of $ErFe_7Al_5$ exhibits intensity enhancements on nuclear reflection positions to be attributed to the occurence of coherent magnetic Bragg scattering as a result of magnetic order. The observed magnetic intensities are in accordance with ferromagnetic spin orientations of both, the Er and the Fe(8f) sublattices. Er and Fe

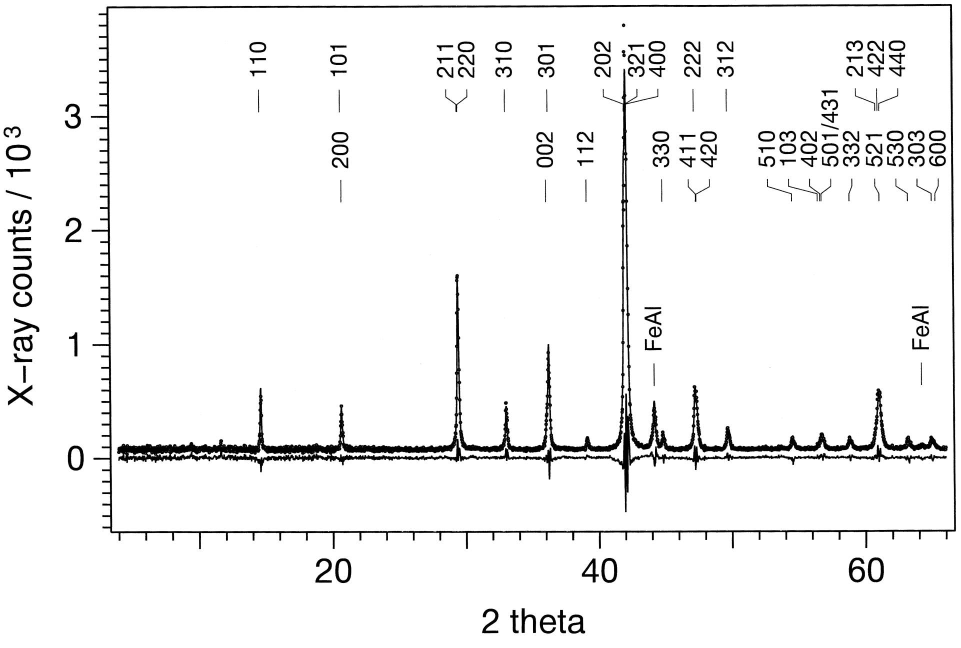

Fig. 1. Rietveld analysed X-ray diffraction pattern of $ErFe_7Al_5$; observations (circles), calculation (line) and differences (line below).

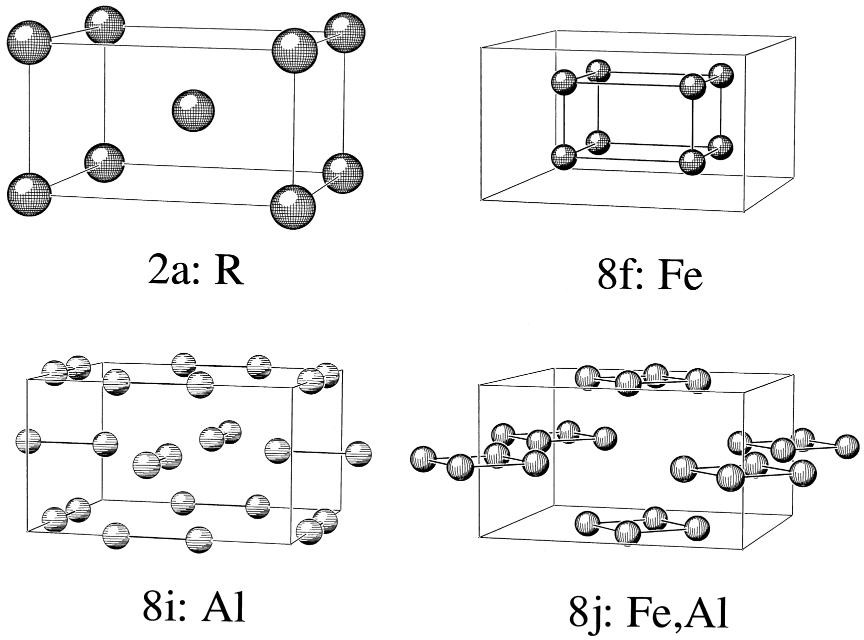

Fig. 2. Partial structures of the $ThMn_{12}$-type structure and site occupations in RFe_7Al_5(R=Er, Y).

Table 1
Lattice parameters *a* and *c*, unit cell volumes *V* and free atomic positional parameters of 8i and 8j sites of $ErFe_7Al_5$ and YFe_7Al_5 according to neutron (n) and X-ray (X) refinements[a]

		$ErFe_7Al_5$			YFe_7Al_5		
		T=4.2 K	*T*=293 K	*T*=400 K	*T*=4.2 K	*T*=293 K	*T*=400 K
a [Å]	n	8.593(3)	8.594(1)	8.613(1)	8.600(2)	8.617(2)	8.629(2)
	X		8.5723(6)			8.636(3)	
c[Å]	n	4.959(3)	4.981(1)	4.985(1)	5.021(1)	5.031(1)	5.040(1)
	X		4.9751(4)			5.022(2)	
V [Å^3]	n	366.2	367.9	369.8	371.4	373.6	375.3
x (8i)	n	0.346(1)	0.342(3)	0.342(2)	0.343(3)	0.345(3)	0.341(2)
	X		0.3545(9)			0.354(2)	
x (8j)	n	0.278(1)	0.278(1)	0.276(1)	0.278(1)	0.278(1)	0.278(1)
	X		0.2719(7)			0.276(2)	

[a] The estimated standard deviations from the Rietveld calculations (in parentheses) are based on measurement statistics and ignore probable systematic errors. R(Bragg)-values are between 0.05 and 0.12.

Table 2
Room temperature interatomic distances [Å] and coordination numbers (co) between the different sites of $ErFe_7Al_5$ (this study) compared to those of $ErFe_6Al_6$ and $ErFe_4Al_8$ according to earlier investigations on the same neutron diffractometer (compare [2])

site–site	co	$ErFe_7Al_5$	$ErFe_6Al_6$	$ErFe_4Al_8$
2a (Er)–8f (Fe)	8	3.248	3.306	3.335
– 8i (Al)	4	2.939	2.973	3.049
– 8j (Fe,Al)	8	3.137	3.194	3.177
8f (Fe)–8f (Fe)	2	2.491	2.521	2.516
– 8i (Al)	4	2.606	2.630	2.665
– 8j(Fe,Al)	4	2.495	2.509	2.533
8i (Al)–8i (Al)	1	2.716	2.697	2.639
– 8j (Fe,Al)	2	2.696	2.716	2.750
8j (Fe,Al)–8j (Fe,Al)	2	2.698	2.775	2.743

spins are oriented antiparallel to each other within the tetragonal basis plane resulting in a ferrimagnetic structure (Fig. 3). The magnetic moment values obtained by an Rietveld refinement of the 4.2 K pattern (Fig. 4) are 8.4(2) μ_B and 2.9(3) μ_B per Er- and Fe-ion at 4.2 K, respectively. The magnetic Fe order is confined to the 8f sublattice. The refinement calculation reveals 0.2(2) μ_B per Fe on the 8j sublattice, i.e. within experimental accuracy no magnetic order on the mixedly occupied 8j site. A control refinement by constraining the Fe moments on 8f and 8j sites resulted in 1.2(1) μ_B per Fe, but led to a deterioration of the magnetic *R*(Bragg)-value from 9.0% to 10.3%.

According to the measured temperature dependences of the strongest magnetic reflections (Fig. 5) the Curie temperature of the transition from paramagnetism to

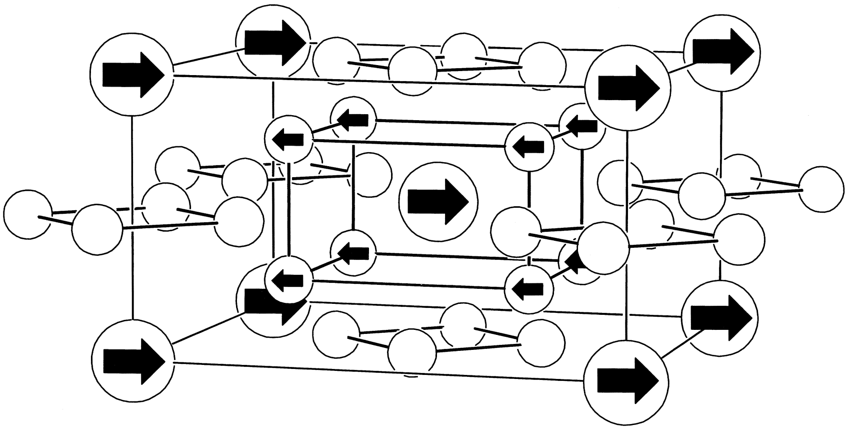

Fig. 3. Ferrimagnetic unit cell of $ErFe_7Al_5$ consisting of ferromagnetically aligned Er moments (large black arrows) and ferromagnetically ordered Fe moments on 8f (small arrows); Fe moments on 8j sites (open circles) are not ordered.

ferrimagnetism is found slightly above room temperature (T_C=320±20 K).

No magnetic Bragg scattering is observed in the low temperature pattern of YFe_7Al_5. The material remains in a state of long range magnetic disorder at least down to 4.2 K.

2.3. Discussion

The structural results of $ThMn_{12}$-type $ErFe_7Al_5$ and YFe_7Al_5 correspond to those of less iron containing $R(Fe_xAl_{1-x})_{12}$ compounds with preferential site occupations of Fe and Al atoms on 8f and 8i sites, respectively, and with statistical distributions of the remaining Fe and Al on 8j sites. This is a confirmation that Fe atoms favour largest possible distances to the rare earths (compare [2]). In $ErFe_7Al_5$, for example, the Er–Fe distances (2a–8f) and (2a–8j) are 3.248 Å and 3.137 Å, respectively, while the distances between Er and Al on 8i are only 2.939 Å (see Table 2). The metallic radii of Fe (1.274 Å) and Al (1.432 Å) rather indicate an inverse site occupation with respect to the distances to R. Due to the actual site occupations, 8f-intrasublattice and (8f–8j)-intersublattice distances between Fe atoms become almost identical by 2.493±0.002 Å and 2.512±0.006 Å in $ErFe_7Al_5$ and YFe_7Al_5, respectively (compare Table 2). Higher iron concentrations, however, cause a gradual reduction of the (2a–8f) distances being 0.087 Å from $ErFe_4Al_8$ to $ErFe_7Al_5$ (see

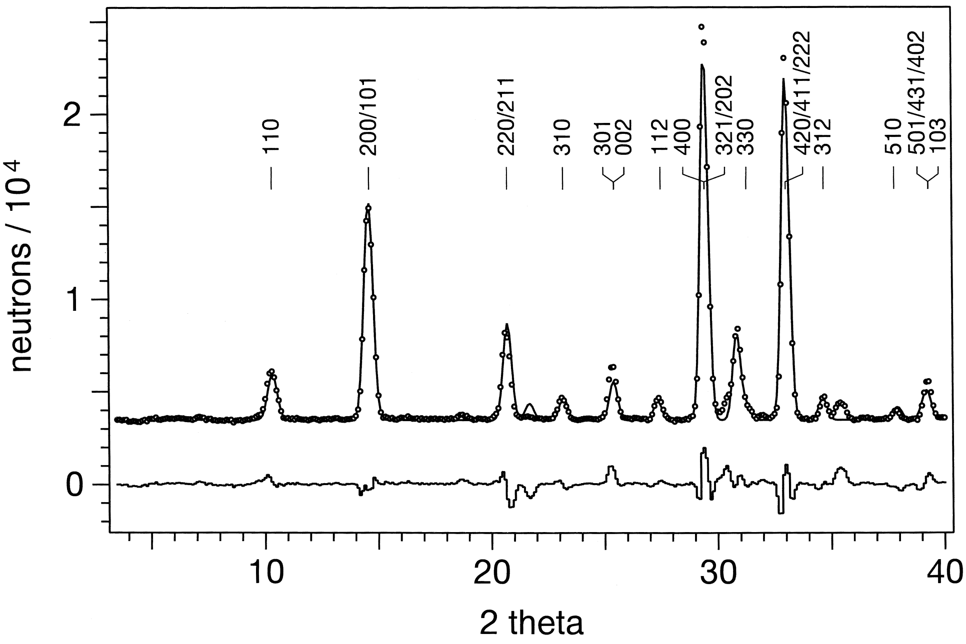

Fig. 4. Front part of the Rietveld analysed 4.2 K neutron diffraction pattern of $ErFe_7Al_5$; observations (open circles), calculation (line) and differences (line below).

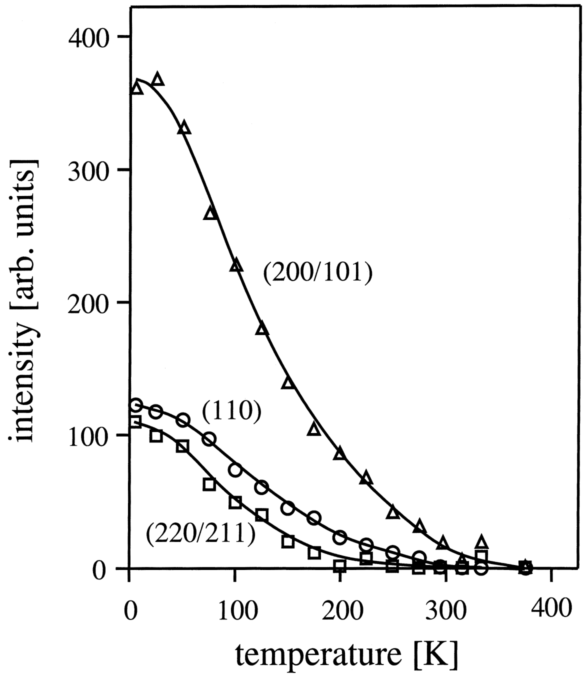

Fig. 5. Temperature dependence of magnetic Bragg intensities according to neutron diffraction; sizes of symbols correspond to experimental standard deviations.

Table 2). This distance reduction is corroborated by the Fe concentration dependent decrease of the unit cell volumes as illustrated in Fig. 6. This decrease is mainly due to the changes of the lattice parameter a as has been observed and discussed also for other $R(Fe_xAl_{1-x})_{12}$ compounds (compare [2]).

The ferrimagnetic structure of $ErFe_7Al_5$ collinear spin orientations within the tetragonal basis plane and antiparallel orientations of Er and Fe spins is identical to the magnetic structures of $ErFe_5Al_7$ [4] and $ErFe_6Al_6$ [3] where, however, Fe on 8j sites is assumed to participate in the magnetic order and where the onset of long range ferrimagnetic order is observed at 62 K and around 340 K, respectively. Strong magnetic coupling between Er and Fe is evident since identical Curie temperatures of around 320±20 K are observed for the ferromagnetic Er and Fe sublattices. The experimental temperature error bar is rather large since the magnetic ordering process is initially developing gradually (Fig. 5). Magnetization saturation is reached only at low temperatures. The Er moment of 8.4(2) μ_B is in reasonable agreement to those reported for $ErFe_6Al_6$ (8.8(2) μ_B) and $ErFe_5Al_7$ (8.9(1) μ_B) [2]. The Fe moment of 2.9(3) μ_B confined to the 8f site is compared to 2.5(2) μ_B and 2.2(1) μ_B in $ErFe_6Al_6$ and $ErFe_5Al_7$, where additional Fe moments of 1.8(1) μ_B each have been found on the 8j sites [2]. The attribution of ordered moments to the 8j sites, however, seems somewhat doubtful with regard to the limited discrimination of the different models by means of neutron powder diffraction.

Despite the comparatively high iron concentration, there is no onset of long range magnetic order occuring in YFe_7Al_5 down to 4.2 K. This leads to the conclusion that (ferri)magnetic order in RFe_7Al_5 compounds is only realized in the presence of strong magnetic coupling and interaction between magnetic rare earth and magnetic iron sublattices. Neutron diffraction experiments on other RFe_7Al_5 compounds are in progress.

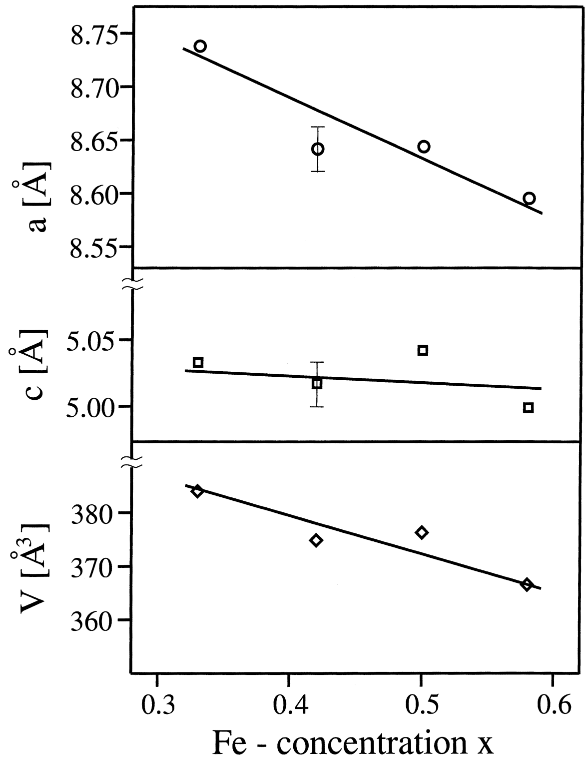

Fig. 6. Room temperature lattice constants a and c and unit cell volumes of $Er(Fe_xAl_{1-x})_{12}$ intermetallics according to neutron diffraction measurements at $x=0.58$ ($ErFe_7Al_5$, this study) and $x=0.50$, 0.42, and 0.33 ($ErFe_6Al_6$, $ErFe_5Al_5$, and $ErFe_4Al_8$, respectively, see [2]).

Acknowledgements

The neutron diffraction experiments were performed under the technical assistance of R. Skowronek. Financial support by the BMBF, Bonn, under contract no. 03-KI5BO2 (neutron diffractometer SV7) is gratefully acknowledged.

References

[1] W. Schäfer, W. Kockelmann, I. Halevy, J. Gal, in: Proc. of EPDIC-6, Budapest, 1998, Materials Science Forum 321–324 (2000) 670–675.

[2] W. Schäfer, W. Kockelmann, A. Kirfel, in: Proc. 1st Int. Conf. on Inorganic Materials, Versailles, 1998, J. Inorg. Mater., in print.

[3] W. Schäfer, W. Kockelmann, S. Fredo, I. Halevy, J. Gal, J. Magn. Magn. Mater. 177–181 (1998) 808–810.

[4] W. Kockelmann, W. Schäfer, G. Will, P. Fischer, J. Gal, J. Alloys Comp. 207/208 (1994) 311–315.

[5] W. Schäfer, W. Kockelmann, G. Will, P. Fischer, J. Gal, J. Alloys Comp. 225 (1995) 440–443.

[6] W. Xian-Zhong, B. Chevalier, T. Burlureau, J. Etourneau, J.M.D. Coey, J.M. Cadiogan, J. Less-Common Metals 138 (1988) 235–240.

[7] W. Schäfer, E. Jansen, R. Skowronek, A. Kirfel, Physica B 234–236 (1997) 1146–1148.